



1 **Quantifying the response of water and carbon balances to land**
2 **cover and climate extremes across Germany.**

3 Karim Pyarali^{1,2*}, Lulu Zhang^{2*}, Ning Liu⁴, Abdulhakeem Al-Qubati^{1,2} and Ge Sun^{3*}

4 ¹Technische Universität Dresden, Helmholtzstr. 10, 01069, Dresden, Germany.

5 ²United Nations University, Institute for Integrated Management of Material Fluxes and of Resources, Ammonstrasse
6 74, 01067, Dresden, Germany.

7 ³Eastern Forest Environmental Threat Assessment Center, Southern Research Station, USDA Forest Service, Research
8 Triangle Park, NC 27709, USA.

9 ⁴CSIRO Environment, Canberra ACT 2601.

10 *Corresponding authors: Karim Pyarali (karim.pyarali@tu-dresden.de); Lulu Zhang (lzhang@unu.edu); Ge Sun
11 (Ge.Sun@usda.gov)

12



Abstract. Land cover and extreme weather events are closely connected to water yield and carbon sequestration. Understanding the tradeoffs between carbon and water and how they respond to human disturbances is critical for quantifying ecosystem services. The monthly scale ecosystem model, WaSSI, was tested and applied across Germany for mapping carbon and water balances from 2001-2019. We estimated that Germany generates 84.86 billion m³ of discharge and sequesters 106.03 Tg of carbon annually. The eastern states were comparatively drier than the rest of the country, as most of their precipitation was lost as evapotranspiration. Croplands, urban areas and Evergreen Needle Forests (ENF) provide 82.5% of the water yield, while the forests sequester the major share of carbon (56.3%) altogether. The results highlight the importance of sparse land covers (e.g. wetlands) in carbon sequestration. Findings also suggest that national water yield and carbon balances are sensitive to extreme events. In 2002 and 2013, due to high precipitation, the stocks of key ecosystem services were notably higher. Similarly, during the drought years of 2003 and 2018, the services were reduced drastically, but we found that buffers from the previous year played an important role in mitigating negative impacts. This study highlights that, when integrated with local data, a relatively simple modelling approach is adequate to answer questions of coupled water and carbon responses to climatic variability at a large scale. We conclude that land management of both forests and croplands are vital to sustain ecosystem services under a changing climate.

1. Introduction

Ecosystem services such as water yield and carbon sequestration are intimately linked with land cover and climate extremes. The two key ecosystem services support life and economic activity (Morales et al., 2005). The tightly coupled links between water and carbon cycles through parameters such as precipitation, temperature, evapotranspiration (ET), and ecosystem services are well recognized (Beer et al., 2007; G. Sun et al., 2011). However, it is still unclear how changes in land cover and climate extremes have impacted these services in Germany at a national level. These services are challenging to measure directly, but an ecosystem services model can be applied to estimate them across the German landscape at a sub-basin scale.

Changes in land cover are driven by multiple interconnected reasons two of them are improving living standards and population growth (Allan et al., 2022). Studies have shown that land cover change greatly reduces ecosystem services, but the impact varies spatially and temporally (Hasan et al., 2020). According to Pandey & Ghosh (2023), and Salerno et al. (2018), urbanization disrupts regulating service for e.g., water purification, soil retention, and climate regulation. On the other hand, Arowolo et al. (2018) and Cui et al. (2021) observed that expansion of cropland often increases goods from provisioning services such as food, fodder and water yield. A recent survey in 2022 from the German national forest inventory found that since 2017 the German forest has become a source of carbon dioxide, instead of being a sink. The reason behind the change in ecosystem functions is the high loss of living biomass due to climate change and low forest growth (Fourth Federal Forest Inventory 2022, 2024).

Another environmental phenomena that impact ecosystem services are extreme climate events (e.g. droughts & floods). Catastrophic weather events not only made countries in the Global South but also in Global North vulnerable. Germany's 2021 summer flood resulted in a loss of 220 lives and US\$ 40 Billion (Schumacher, 2022); the incurred damages from the 2003 drought, primarily on agriculture, were approximately US\$13 Billion across Europe (Eisenreich, 2005). Germany has seen an increase in the intensity and frequency of heavy rainfall, more in winter than summer, the air temperatures are also projected to rise by 1.6 to 3.8°C by 2080 (Schröter et al., 2005). A shift in precipitation season has been observed, which will potentially increase the risks of floods during winter and decrease the water supply during summer periods (Schröter et al., 2005). The extreme events are changing due to climate change. Their impacts may reduce terrestrial carbon uptake or gross primary productivity (GPP) (Williams et al., 2014). Which negatively affects other factors within the co-evolved processes of carbon-water cycle in an integrated terrestrial system (L. Zhang et al., 2018). Potentially leading to adverse effects on regional food and livelihood security.

Although ecosystem services are essential and well-recognized in Germany, national-scale studies on both carbon and water yield are still lacking. There are multiple studies that focus on a specific land cover type or specific ecosystem services at the European, national or subnational scales. For example, Potter & Pass (2024) estimated the changes in net primary productivity (NEP or carbon sequestration) for Western Europe, including Germany. Gutsch et al. (2018) assessed German forest ecosystem services under climate change and different management scenarios. Their results



showed that climate change has negative impacts on water percolation and positive impacts on carbon sequestration. Using agricultural long-term field experiments, carbon sequestration was projected to increase in the southern parts of Germany, indicating higher productivity, and decrease in central and east Germany where poor soil will further reduce the productivity (Donmez et al., 2024). Other studies used regional analysis to assess water or carbon cycles (Al-Qubati et al., 2023; Prescher et al., 2010; Ungaro et al., 2021; Wu et al., 2021). The lack of integrated water-carbon cycles assessment hampers deriving national or regional adaptive land management strategies to alleviate the adverse impacts resulting from environmental and climate change, particularly in the long term.

Furthermore, we observed a varied response of the coupled water-carbon cycle to changes in land cover and climate (Cheng et al., 2017; Jung et al., 2017; Zeng et al., 2018). The variation is manifested by the coupled mechanisms occurring at multiple timescales. These may be short-term leaf-gas exchanges, monthly or annual ET and carbon accumulation, and long-term water yield and species composition. This emphasizes that a single type of observation is not sufficient to provide the robust validation needed to address the response of water and carbon cycles to environmental disturbances or climate shocks (Margulis et al., 2006). Gentine et al. (2019) argued that terrestrial water-carbon cycles must be investigated as an integrated system. They recognized the importance of incorporating multiple observations on different timescales from various sources to better validate model simulations, which may reduce uncertainties, mitigate bias, and provide better predictions. Unfortunately, the suggested approach is seldomly applied in hydrological modelling (e.g. G. Sun et al., 2011, 2023; J. Zhang et al., 2022; Y. Zhang et al., 2016). Thus, impeding the improvement of our predictive ability to quantify the potential water-carbon changes and consequences that are vital to effective policy decision-making for developing climate adaptation and mitigation strategies. Therefore, we integrated multi-timescale observations and information sources in our model to validate simulated water yield and carbon sequestration. We used gauged river discharge (Q), in-situ measured ET and GPP from eddy flux towers, and remotely sensed ET and GPP data for model validation.

In this study, the Water Supply Stress Index (WaSSI), an ecosystem service model, was applied on a monthly resolution to simulate the water and carbon process across the different land covers within Germany (G. Sun et al., 2011). The model has been used globally for various purposes and under different climatic and socioeconomic conditions (Averyt et al., 2011; Caldwell et al., 2011, 2014, 2012; N. Liu et al., 2020; G. Sun et al., 2011; S. Sun et al., 2015) in the United States of America, Rwanda, Australia, and China (N. Liu, 2017; N. Liu et al., 2013; McNulty et al., 2016; G. Sun et al., 2011). By validating the WaSSI model, we aim to have an improved understanding of the response of water-carbon cycles on German land cover with climate variability at a watershed scale. Furthermore, we focus on three questions: (i) How did ET, water yield and NEP vary over time and space (ii) how did different land cover contribute to water yield and carbon sequestration? and (iii) to what extent and how sensitive are the two ecosystem services to extreme weather events (i.e., droughts and floods)?

2. Methodology and Data

The WaSSI model merges the water and carbon cycle using water use efficiency (WUE) parameters estimated from global eddy flux observations. It is made up of two components: a hydrological and a carbon sub-model. The required inputs are precipitation, temperature, digital elevation model, land cover, fractional impervious cover, leaf area index (LAI), and soil parameters, while the outputs are Q, ET, GPP, and net ecosystem exchange (NEE) (N. Liu, 2017). Transboundary inflows and outflows were not accounted in this study, therefore, watersheds close to Germany's boundary, which accumulated their flow across the border, were not considered.

The WaSSI model estimates land cover specific water yield (mm per month), which can be aggregated as flow volume down streams (m^3 per month) for any individual watersheds. The hydrologic fluxes estimated are snow melt, snow accumulation, soil storage, surface flow, base flow, routed flow accumulation, and ET (G. Sun et al., 2011). The model employs a conceptual method (McCabe & Wolock, 1999) that uses the monthly average temperature and mean average elevation of a watershed to partition precipitation into rainfall and snowfall, estimate the rate of snow melt and calculate the mean monthly snow water equivalent for each watershed (Caldwell et al., 2012). The Sacramento Soil Moisture Accounting (SAC-SMA) model was used for soil and runoff parameters, which runs infiltration, baseflow, surface runoff, and soil moisture processes, while also constraints ET estimates based on soil water content. For ET estimations, we used the Type II regression model from (Fang et al., 2016), where the ET model was developed using



109 quality-controlled global data from more than 200 eddy flux sites, incorporating the three most commonly available
110 biophysical parameters precipitation (P), potential ET (PET) and LAI in the following equation:

$$ET = -4.79 + 0.75PET + 3.92LAI + 0.04P \quad (1)$$

111 WaSSI estimates three main components of the carbon cycles: (i) GPP or total carbon uptake, (ii) ecosystem
112 respiration (Re) representing carbon loss, and (iii) NEP or negative NEE or carbon sequestration. Equation 2 estimates
113 the amount of NEP by subtracting Re from GPP.

$$NEP = -NEE = -(Re - GPP) \quad (2)$$

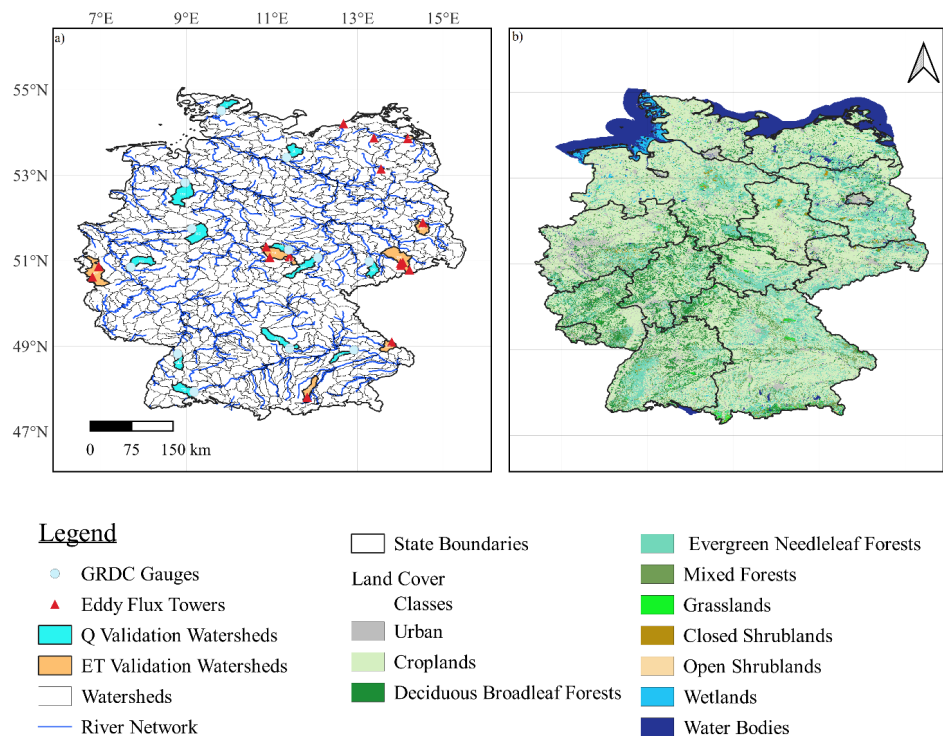
114 Furthermore, a closely coupled relationship between ET and GPP has been found in multiple studies (Law et al., 2002;
115 G. Sun et al., 2011), as presented in Equation 3. GPP is linearly correlated to ET and land cover specific WUE
116 parameters were estimated using 142 eddy flux tower data (Y. Zhang et al., 2016). Similarly, the Re from heterotrophic
117 and autotrophic bacteria can be estimated using Equation 4, where regression coefficients are estimated from eddy
118 flux data. The coefficient (a, m, and n) values used in this study are provided in Table S1 in the supporting documents.

$$GPP = a \times ET \quad (3)$$

$$Re = m + n \times GPP \quad (4)$$

119 2.1. Model Validation

120 We validated the model outputs using both in-situ observed data (e.g., stream discharge data from gauge stations and
121 ET eddy flux data) and remotely sensed data (e.g., ET and GPP estimates from satellites). Initially, the discharge was
122 validated for twelve upstream watersheds across Germany, (Fig. 1). The performance criteria to determine the
123 accuracy of monthly outputs are model bias (%), R^2 , scatter plots, Nash-Sutcliffe efficiency (NSE), and Kling-Gupta
124 efficiency (KGE). The estimated ET was validated against several timescale data, including daily eddy flux, monthly
125 MODIS ET, and watershed-specific water balance values calculated by subtracting Q from precipitation on a monthly
126 and annual timescale. For carbon, we compared the GPP estimates with GPP measurements from eddy flux towers,
127 MODIS GPP, and CGLS GPP.



128

129 **Figure 1:** A map of the study area presenting **a)** Germany's boundaries with all the 804 watersheds delineated, Global
130 Runoff Data Center's (GRDC) gauge station locations, major rivers, eddy flux tower sites and representative
131 watersheds for Q and ET validation and **b)** Germany's land cover and state boundaries.

132 2.2. Input Data

133 2.2.1. Climate Data

134 Climate data (i.e., precipitation and temperature) is sourced from Germany's national meteorological service (DWD,
135 2018). Datasets have a spatial resolution of 1km and a temporal resolution of months. The gridded data are prepared
136 by estimating monthly deviations for each station, which are then interpolated using inverse squared distance weighted
137 interpolation and transformed back into real values using reference grids (Kaspar et al., 2013).

138 2.2.2. Land cover classification

139 CORINE land cover (CLC) map of 2018 with a 100m spatial resolution was used in this study (EEA, 2021). Validation
140 studies showed that it can capture land cover with an accuracy of 85% (Büttner et al., 2021; Keil, 2017). This study
141 reclassified land cover into 10 major classes to reduce complexity. Table S2 shows the range of CLC classes that were
142 merged along with their percentage across Germany.

143 2.2.3. Leaf Area Index

144 Climate Data Record's (CDR) Vegetation (VGT) sensor LAI was used. The data is available from 2001 to 2014, with
145 a 10-day temporal and 1km spatial resolution. All pixels with an invalid LAI status were removed during quality
146 control (Verger et al., 2018). Validation studies of this product showed that it underestimates ground data with a bias
147 of 0.31 and a correlation of 0.72, while against multiple satellite datasets, it overestimates with biases ranging between
148 0.03 (for MODIS) to 0.36 (for GLOBCARBON) (Camacho & Cernicharo, 2014).



149 **2.2.4. Fractional impervious cover and soil data**

150 The fractional impervious cover is derived from the Global Man-made Impervious Surface (GMIS) dataset (Brown
151 de Colstoun et al., 2017). It has a spatial resolution of 30m.

152 Digital soil map BUEK 200 was used to estimate eleven soil parameters following Y. Zhang et al. (2011) and Anderson
153 et al. (2006). Land cover and soil properties were used to obtain the curve number (CN) that controls the partitioning
154 of soil into upper and lower zones. The water allocation between tensed and free water storage is determined by soil
155 composition. The final product has a spatial resolution of 500 m.

156 **2.3. Validation Data**

157 **2.3.1. Stream Discharge Data**

158 The discharge data used for validation are sourced from the Global Runoff Data Center (GRDC). Twelve upstream
159 stations were identified from a large group of stations for validation of discharge in this work because upstream
160 watersheds have less anthropogenic influences. The stations were selected for different regions of Germany to ensure
161 different land uses and land covers were validated. The location of stations can be observed in Fig. 1, while their
162 names and ID are provided in Table S3.

163 **2.3.2. Eddy Flux ET and GPP**

164 ET and GPP in-situ measurements were acquired from the FLUXNET2015 database. The data available is quality
165 controlled and the gaps within the data are filled and corrected to offer high-quality information. Energy balance
166 closure correction factors (EBC_CF) were used to correct these datasets. The EBC_CF were estimated using three
167 different methods each assuming that the Bowen ratio holds true. In this study, monthly latent heat turbulent flux (LE)
168 was converted to ET with and without energy closure corrections and GPP was calculated using the daytime
169 partitioning method (Pastorello et al., 2020).

170 **2.3.3. MODIS ET and GPP Data**

171 The Moderate Resolution Imaging Spectroradiometer (MODIS) ET product MOD16A2GF is employed in this work.
172 The remote sensing data is used to compare the spatial variation of model output. MODIS has a spatial resolution of
173 500m and a temporal resolution of 8-day. The ET estimation follows the Penman-Monteith equation (Running et al.,
174 2019b). The product has been comprehensively validated in multiple studies (Kim et al., 2012; Z. Liu et al., 2015;
175 Trambauer et al., 2014; Velpuri et al., 2013) and used to evaluate the output of hydrological models (G. Sun et al.,
176 2011). This study used a monthly sum of ET values and spatial average calculated on a sub-watershed scale.

177 The gap-filled GPP product employed in this study is MOD17A2HGF, with a spatial resolution of 500m and a
178 temporal resolution of 8-day. It follows Monteith's logic and uses land cover specific light use efficiency (ϵ), fraction
179 of absorbed photosynthetically active radiation (FPAR), incident photosynthetically active radiation (IPAR), the
180 deficit of vapor pressure, and minimum air temperature (Running et al., 2019a). Insights on the application and
181 validation of MOD-GPP are provided in multiple studies (Z. Liu et al., 2015; G. Sun et al., 2011; Turner et al., 2006;
182 Wang et al., 2017; Zhu et al., 2018).

183 Copernicus Global Land Service (CGLS) GPP are derived from the Gross Dry Matter Productivity (GDMP) values.
184 We used the version 2 product from SPOT/VGT and PROBA-V satellites to evaluate the model GPP estimates for the
185 period of 2001 – 2019. The GDMP product has a spatial and temporal resolution of 1km and 10-day. It represents the
186 additional gross dry biomass stored in vegetation, which could be converted into gross carbon uptake by multiplying
187 it with a scaling factor of 0.45 gC/gDM, as shown in the following equation (Smets et al., 2019).

$$GPP (gC m^{-2} day^{-1}) = GDMP (kg DM ha^{-1} day^{-1}) * 0.45 * 0.1 \quad (5)$$



188 **3. Results**

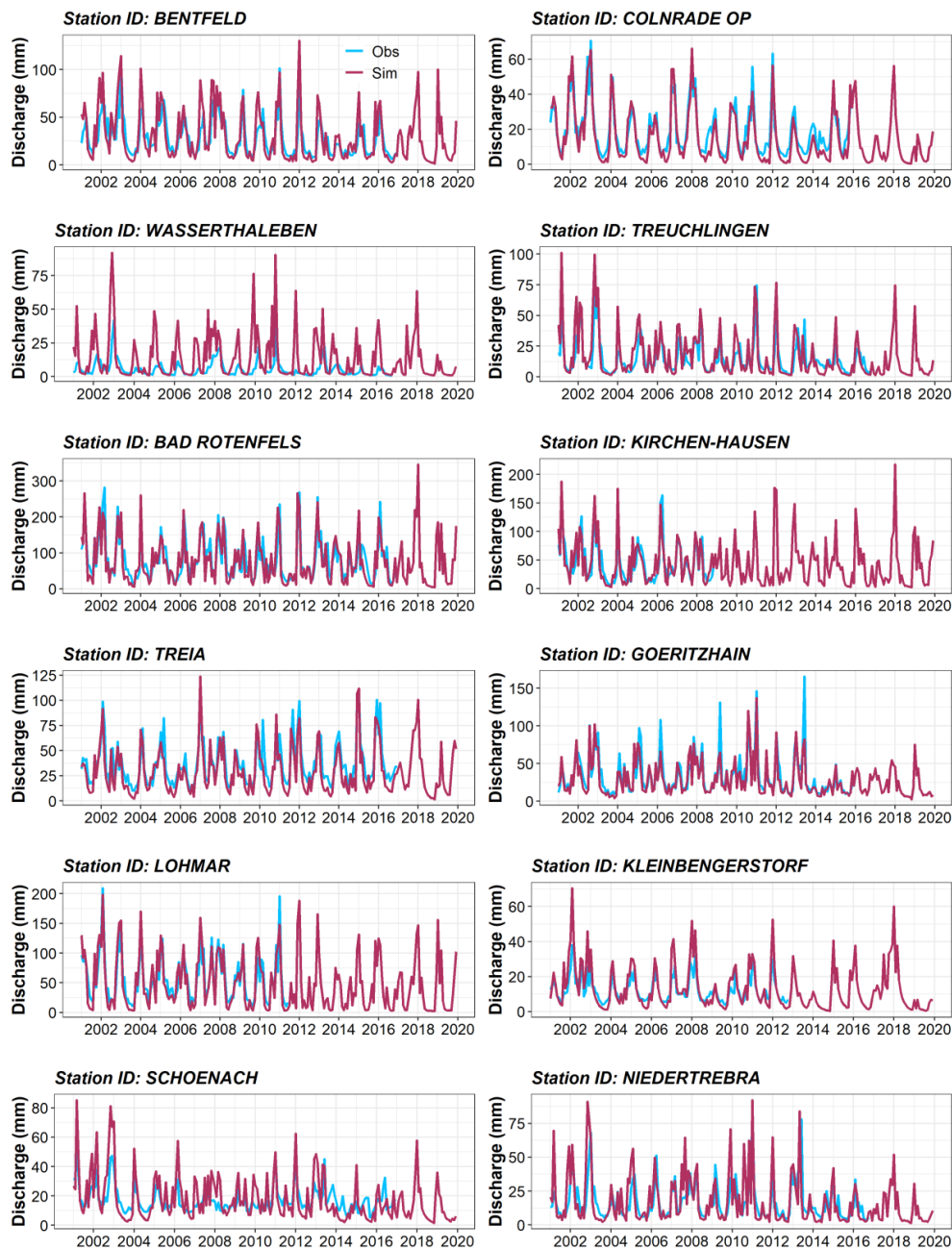
189 **3.1. Model Validation**

190 **3.1.1. Discharge Validation**

191 Model discharge validated on a monthly scale gives Kling-Gupta efficiency (KGE) for eight out of the twelve
192 watersheds above 0.5 and NSE for six out of twelve watersheds greater than 0.6, as shown in Table S3. While on an
193 annual scale the values of model bias (%) for eleven out of the twelve stations were between -25% to 25% and for R^2
194 ten out of twelve stations were above 0.60, as presented in Table S4. The scatter plot between modelled and observed
195 discharge, across the twelve watersheds on both annual and monthly scales, is presented in Fig. S1. The plot showed
196 high correlation between the two datasets suggesting the model performed reasonably well. Furthermore, the
197 hydrograph plots revealed that the model, in general, was able to simulate the monthly flows reasonably well, as
198 shown in Fig. 2. Except for the Wasserthaleben station, where the model performance was weak with bias equal to
199 131.8 % and annual R^2 of 0.18.



200



201

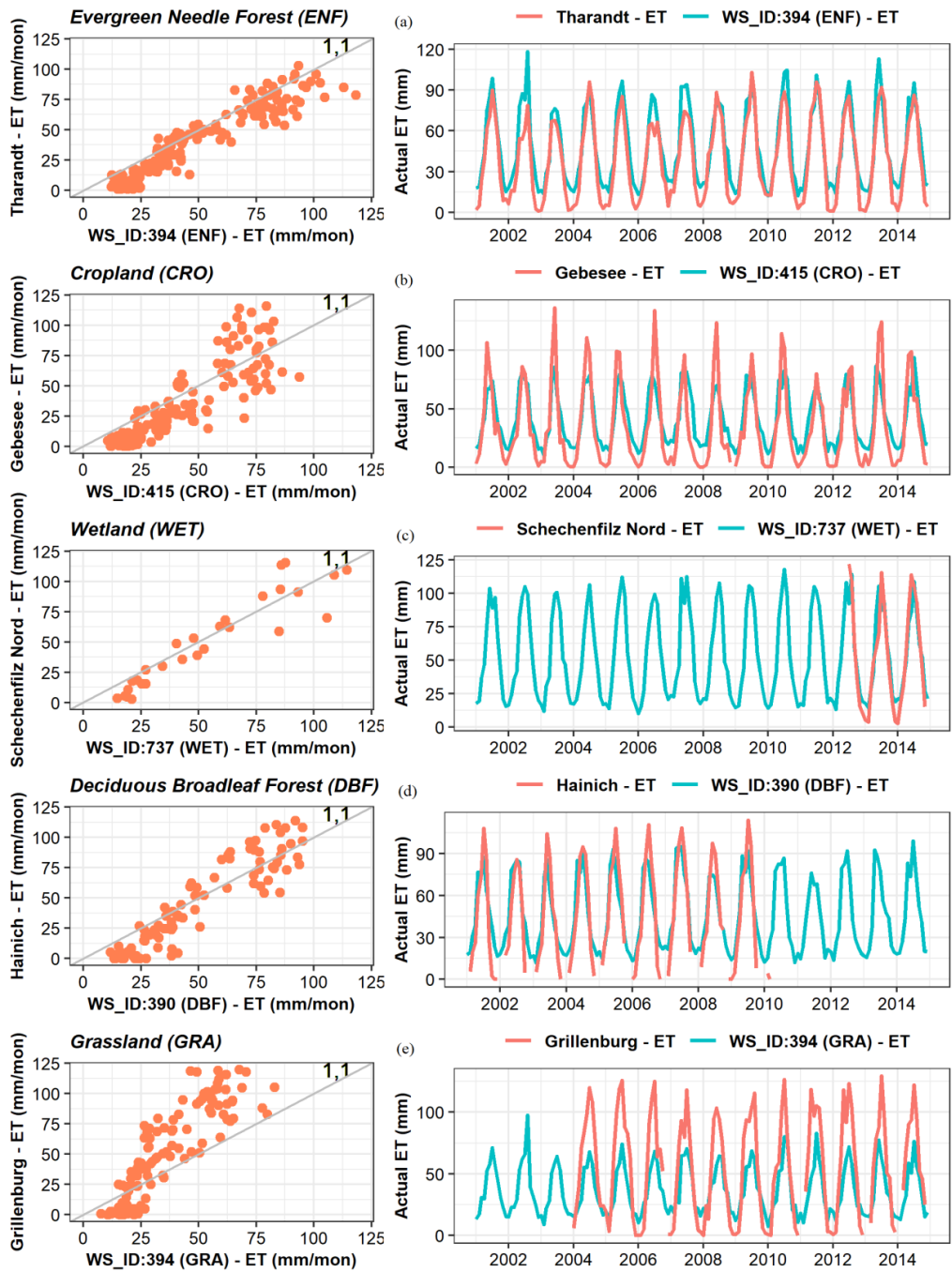
202 **Figure 2:** Monthly discharge time series from WaSSI simulation in mm (maroon) plotted against observed gauge
203 station flow in mm (blue) during 2000-2020.



204 3.1.2. ET Validation

205 The ET estimates from WaSSI were compared with multiple eddy flux (EC) ET observations that are available within
206 Germany. Monthly land cover specific validation of simulated ET against EC ET is presented in Fig. 3. The ET
207 estimates were captured reasonably well by the model as the points in the scatter plot generally stayed close to the 1:1
208 line except for Grassland. The detailed validation results are provided in Table S5. Ten out of eleven watersheds had
209 an R^2 value > 0.6 and a correlation > 0.75 . Seven out of eleven watersheds had a model bias (%) between -25% to
210 25%, and KGE estimate ≥ 0.6 . The greatest discrepancy in this validation was found in Lackenberg with a bias of 52.4
211 %. Overall, the model was able to capture ET values reasonably well across different land covers within Germany
212 (Fig. S2a).

213 WaSSI ET on an interannual scale showed that it can satisfactorily simulate the variability of ET captured by MODIS
214 across Germany, as shown in Fig S2b-c. The model mostly underestimated ET in southern and northwestern Germany,
215 while slightly overestimating the ET in mid-western and eastern Germany. When the simulated ET was assessed
216 against ET estimates as precipitation minus observed discharge ($P - Q_{\text{observed}}$) interannually, the mean annual biases for
217 all the twelve watersheds were within $\pm 25\%$ threshold. Eight out of the twelve watersheds had biases within $\pm 10\%$,
218 indicating a very good model performance (Table S6).



219

220 **Figure 3:** Land cover specific simulated ET validation (WS_ID) against corrected eddy flux ET data. The line running
221 diagonally through the scatter plot is a 1:1 line.



3.1.3. GPP Validation

A monthly land cover specific validation was conducted between modelled GPP and observed GPP from EC towers. The observed GPP estimates were developed using the daytime partitioning method (GPP_DT_VUT_REF). The results showed that nine out of fourteen watersheds had a model bias within $\pm 25\%$, twelve had $R^2 > 0.6$, seven had $NSE > 0.5$, six had $KGE > 0.5$, and all the watersheds had a correlation > 0.6 , as shown in Table 1. Furthermore, the results showed that simulated GPP from WaSSI were higher compared to the remotely sensed GPP estimates from Copernicus and MODIS satellite by approximately 7% and 16%, respectively. The difference, correlation and regression between simulated GPP and remotely sensed GPP is shown in Fig. S3.

Table 1: Monthly validation of WaSSI-GPP against EC-GPP. Stations are grouped for different land covers e.g. cropland (CRO), deciduous broadleaf forest (DBF), ENF, grassland (GRA) and wetland (WET).

Eddy Flux Tower	Watershed ID	Land cover	Model bias %	R^2	Corr	NSE	KGE
Selhausen Juelich	457	CRO	-15.94	0.65	0.81	0.45	0.33
Klingenberg	394		8.34	0.38	0.62	0.37	0.37
Gebsee	415		13.54	0.48	0.69	0.41	0.35
Hainich	390	DBF	8.28	0.84	0.92	0.73	0.57
Leinefelde	390		3.19	0.87	0.93	0.75	0.57
Lackenberg	631	ENF	224.09	0.83	0.91	-5.82	-1.51
Oberbärenburg	394		-13.4	0.86	0.93	0.74	0.59
Tharandt	394		-19.7	0.89	0.94	0.73	0.59
Grillenbourg	394	GRA	-35.42	0.75	0.87	0.37	0.3
Rollesbroich	457		-26.79	0.81	0.9	0.55	0.49
Schechenfilz Nord	737	WET	2.61	0.68	0.83	0.67	0.82
Spreewald	269		-50.54	0.82	0.91	0.18	0.16
Zarnekow	38		21.62	0.84	0.92	0.77	0.7
Anklam	23		-40.91	0.63	0.79	0.28	0.2

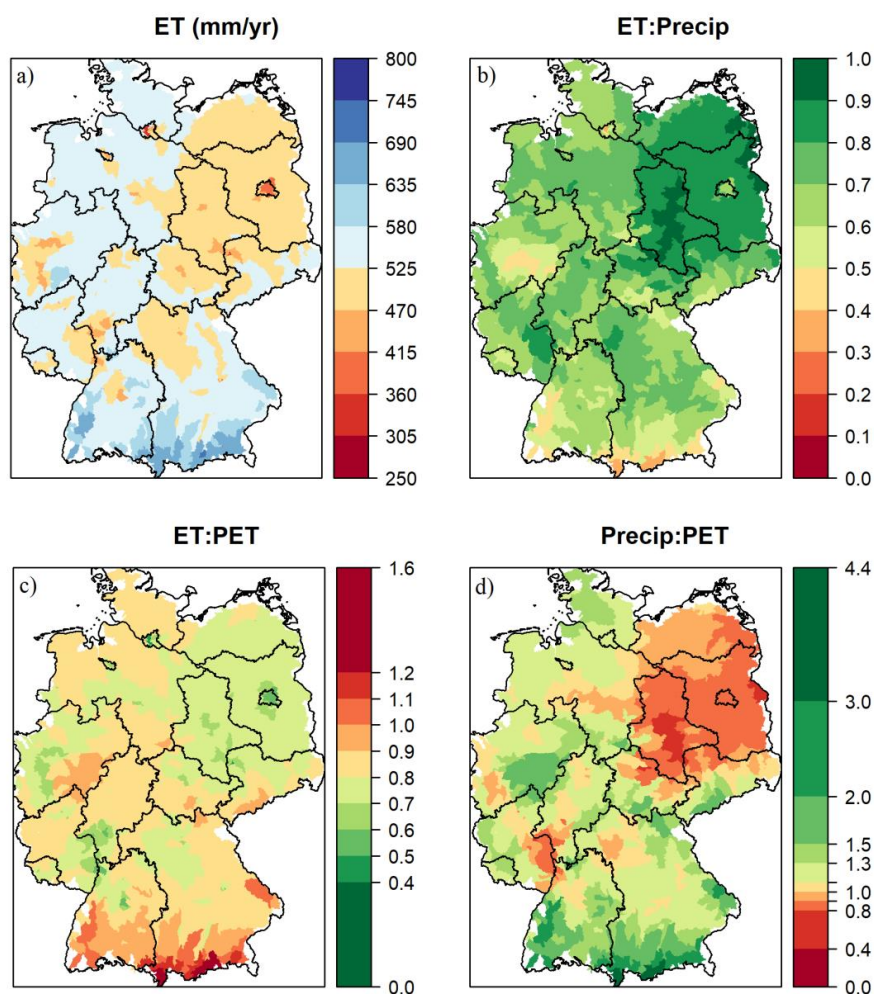
3.2. Understanding the water-carbon coupling across Germany

3.2.1. Spatial variation of ET from 2001 - 2019

Over a nineteen-year period, the mean annual ET across Germany ranged between 250 to 800 mm yr⁻¹ and had a spatial mean and standard deviation of 530 ± 49.5 mm yr⁻¹. Eastern Germany (Saxony Anhalt, Brandenburg, Mecklenburg Vorpommern, Saxony, and Thuringia) had lower ET than the spatial mean, while the South and West



239 had higher ET, as shown in Fig. 4a. On an annual scale, Bavaria and Lower Saxony experienced significant ET losses.
 240 The absolute losses were 39.5 billion $\text{m}^3 \text{yr}^{-1}$ in Bavaria and 25.7 billion $\text{m}^3 \text{yr}^{-1}$ in Lower Saxony. Bavaria had a
 241 smaller fraction of its precipitation lost as ET (0.3 to 0.9) compared to Lower Saxony (0.5 to 0.9). Across Germany
 242 the eastern states lost the largest share of their precipitation as ET (0.8 – 1.0), leading to a very limited available water
 243 supply in the region, shown in Fig. 4b. Furthermore, to understand whether ET is limited by energy or water
 244 availability, we estimated ET:PET ratio across Germany. The actual ET of watersheds near the Alps exceeds the PET.
 245 These watersheds receive more precipitation compared to the rest and thus energy limits the ET values, while the
 246 water availability limits ET for the rest parts of Germany (Fig. 4c). Lastly, eastern states and some watersheds in
 247 Rhineland-Pfalz and Hessen are drier with relatively high-water scarcity as they receive less precipitation compared
 248 to their PET (Fig. 4d).



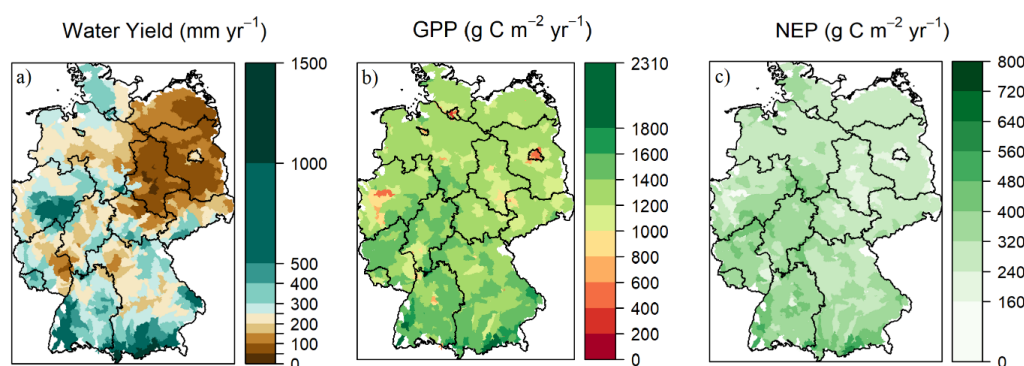
249

250 **Figure 4:** Modelled parameters presenting ET dynamics on a watershed scale across Germany over state boundaries
 251 within the period of 2001 - 2019. The separate sections show a) mean annual actual ET (mm yr^{-1}), b) ratios between
 252 ET and precipitation, c) ratios between ET and potential ET and d) ratios between precipitation and potential ET.



3.2.2. Ecosystem services across Germany throughout 2001 – 2019.

The mean annual water yield across Germany ranges between $31.8 - 1477.5 \text{ mm yr}^{-1}$, has a spatial average of $259 \pm 173.5 \text{ mm yr}^{-1}$ and generates a total discharge of 84.86 billion m^3 per year (Fig. 5a). In eastern states the water yield was lower than the spatial average, while in southern states it was higher. The mean annual GPP estimates (Fig. 5b) were found between $0 - 2046.5 \text{ g C m}^{-2} \text{ yr}^{-1}$ with a spatial average of $1278.8 \pm 237.7 \text{ g C m}^{-2} \text{ yr}^{-1}$ and a total national carbon uptake of $441.54 \text{ Tg C yr}^{-1}$. The mean annual NEP values (Fig. 5c) were observed between $0 - 665.5 \text{ g C m}^{-2} \text{ yr}^{-1}$ with a spatial average of $308.3 \pm 78.2 \text{ g C m}^{-2} \text{ yr}^{-1}$ and a total national carbon sequestration of $106.03 \text{ Tg C yr}^{-1}$.

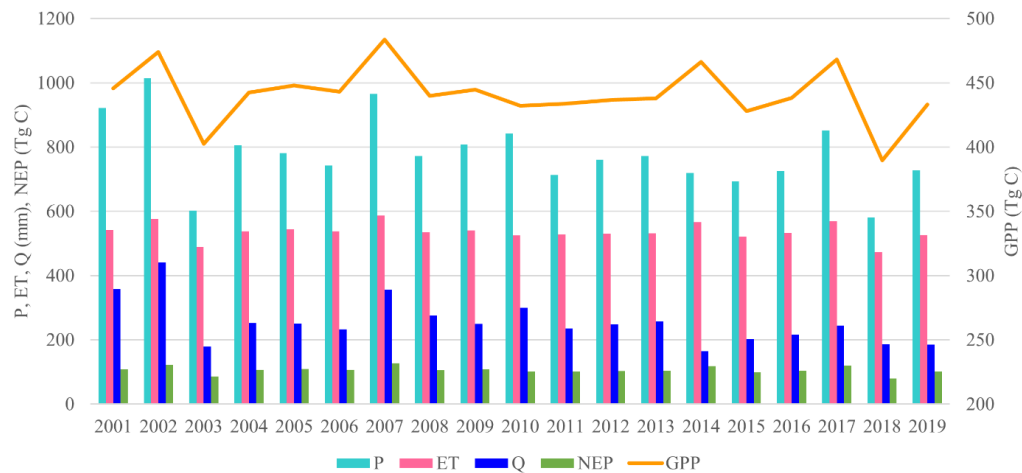


260

Figure 5: Spatial distribution of model simulated **a)** mean annual total water yield (mm yr^{-1}), **b)** mean annual GPP ($\text{g C m}^{-2} \text{ yr}^{-1}$), and **c)** mean annual NEP ($\text{g C m}^{-2} \text{ yr}^{-1}$).

3.2.3. Temporal variability of ecosystem services and the control of land cover on these services.

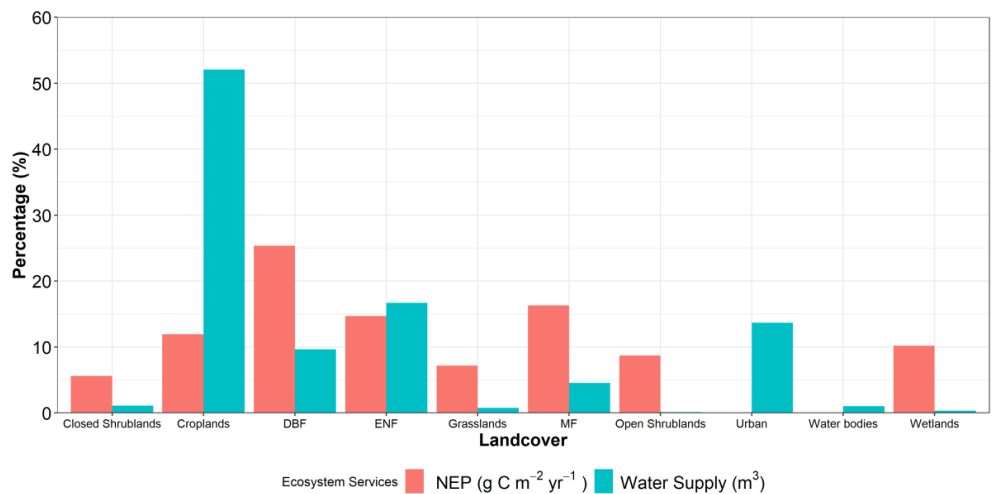
The mean annual precipitation for the period 2001–2019 was estimated at $779 \pm 106.2 \text{ mm/year}$. Notably, 2002 and 2007 were identified as the two wettest years within this timeframe. Precipitation in 2002 exceeded the mean by 30.2%, while in 2007 it was 24% higher than the mean. Conversely, the driest years were 2003 and 2018, with rainfall falling below the mean by 22.7% and 25.5%, respectively. There were relatively high variations in Q and NEP during these wet and dry years, indicating that these two fluxes are sensitive to changes in precipitation compared to ET and GPP. In 2018, which is the driest year in the study period, we observed that compared to the mean there was 25.5% less precipitation. This was accompanied by 11.7% less ET, a 26.8% reduction in Q, 11.7% less GPP and 24.7% lower NEP. Alternatively, during 2002, the wettest year in our study, we found 30.2% more precipitation compared to mean. Which may have lead to 7.4% more in ET, 73.4% higher Q, 7.3% more GPP, and 15.5% rise in NEP, relative to mean. An annual overview for temporal variation is presented in Fig. 6.



274

275 **Figure 6:** Ecosystem fluxes (Precipitation, ET, NEE, GPP) across Germany simulated by the model from 2001 - 2019
276 to observe annual variation.

277 To evaluate the role of land cover in water yield and carbon sequestration, we estimated the share of ecosystem services
278 provided by the ten different land cover classes. The most essential land covers that provide the largest share of water
279 across Germany are Cropland (52.1%), ENF (16.7%), and Urban (13.7%); they supply 82.5% of the water in total.
280 The land covers that sequester most carbon are DBF (25.3%), mixed forest (MF) (16.3%), and ENF (14.7%); they
281 contribute 56.3% of carbon sequestered in Germany. Lastly, we would like to highlight that a small portion of land
282 covers, such as wetlands, open shrubland, closed shrubland, and grasslands cover less than 2% of German territory;
283 however, they regulate > 30% of the total carbon sequestered in Germany, indicating the high importance of
284 conserving these ecosystems, as shown in Fig. 7.



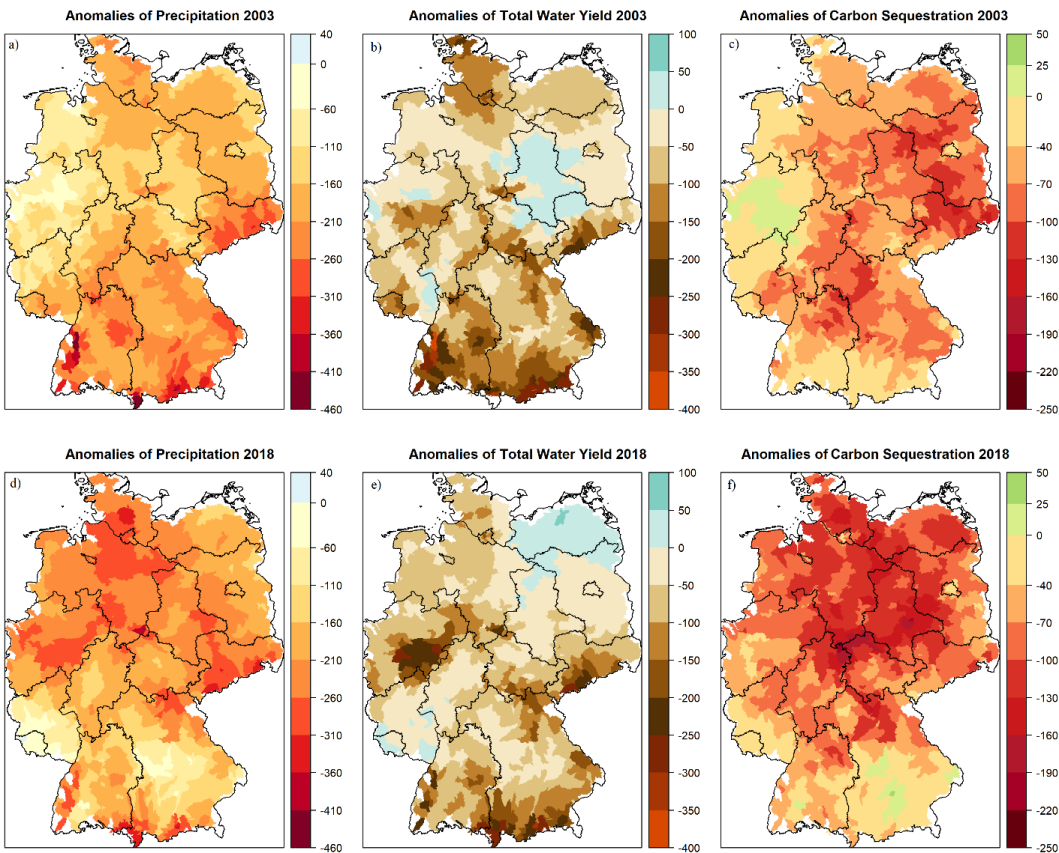
285

286 **Figure 7:** The mean percentage or share of carbon sequestration and water supply originating from different land
287 covers across Germany.



288 **3.2.4. Spatial variability of ecosystem services during extreme weather events**

289 To understand the impact of droughts and floods on ecosystem services, we examined the droughts for the year 2003
290 & 2018 and the floods for the year 2002 and 2013. During 2003, precipitation was 22.7% less than its average and
291 only western states had close to average precipitation. The total water yield was 29.6% less than average. The carbon
292 sequestration was 18.5% lower than average. While western states had close to average carbon sequestration the rest
293 experienced significantly reduced levels. Compared to 2003, the pattern and intensity of the 2018 drought was more
294 severe. During this event, Germany cumulatively received 25.5% less precipitation, had a 26.8% lower water yield,
295 and had 24.7% less carbon sequestration. The total water yield was 62.13 billion m³, total carbon uptake was 389.77
296 TgC, and total carbon sequestration was 79.82 TgC. The variations in ecosystem services due to both drought events
297 are presented in Fig. 8. On the other hand, during the extremely wet year of 2002, Germany received 30% more
298 precipitation than annual mean. The water yield and carbon sequestration were 70% and 15.5% higher than the mean,
299 respectively. The second wet year of 2013 suffered from severe regional floods. The regions that received higher
300 precipitation had a larger water yield and sequestered more carbon. Interestingly, northwest Germany was drier than
301 the mean, as a result the overall ecosystem services for 2013 were close to the mean estimates. The variations in
302 ecosystem services during both years are presented in Fig. 9.



303 **Figure 8:** The response of ecosystem services (water yield (mm) and carbon sequestration (g C m⁻²)) during two
304 drought events (2003 and 2018). Both drought events had different spatial patterns and intensities, thus the response
305 from the ecosystem varied spatially. The anomalies in the figure were estimated by subtracting the mean annual values
306 for the period 2001 – 2019 from the estimates of the individual drought years 2003 and 2018 on a watershed scale.
307

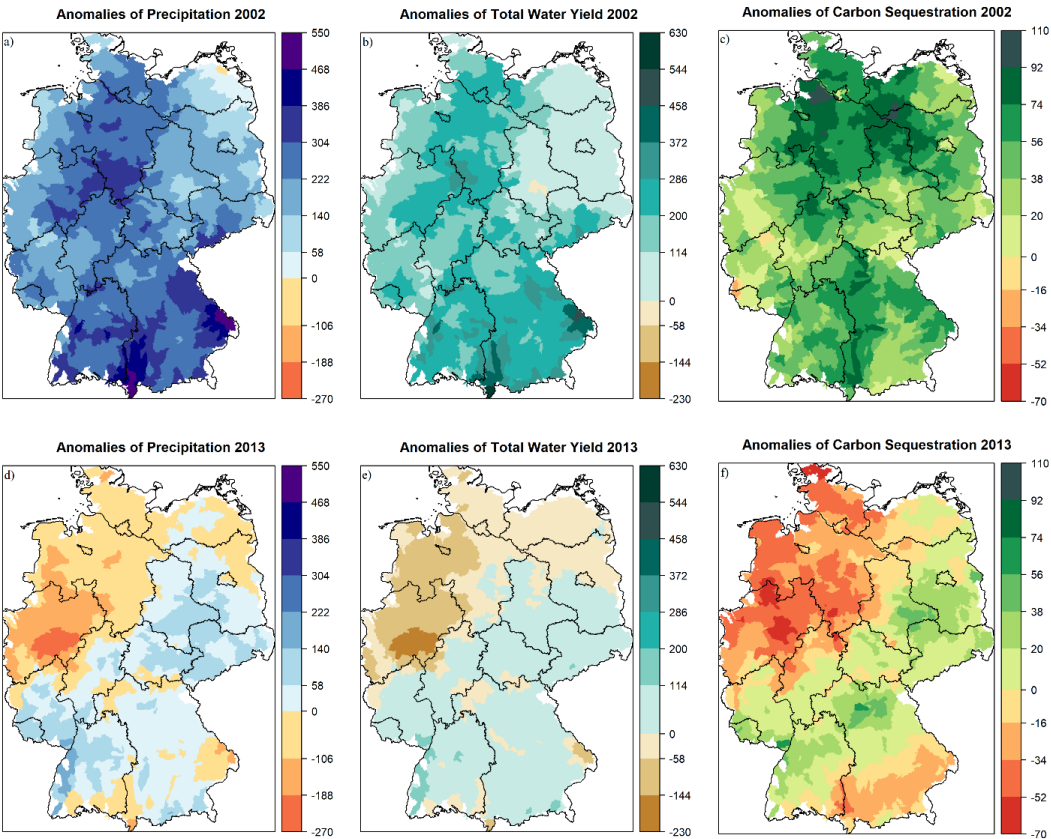


Figure 9: The response of ecosystem services (water yield (mm) and carbon sequestration (g C m^{-2})) during two flood events (2002 and 2013). Both events had different spatial patterns and intensities, thus the response from the ecosystem varied spatially. The anomalies in the figure were estimated by subtracting the mean annual values for the period 2001 – 2019 from the estimates of the individual year 2002 and 2013 on a watershed scale.

4. Discussion

This study explores the response of water-carbon cycle to land cover and extreme events across Germany on watershed scale. The WaSSI model performs reasonably well in this region and is estimated to generate 84.86 billion m^3 of discharge and 106.03 TgC of carbon sequestration per year. The results also highlight the importance of sparse landcovers (e.g. wetlands, open shrubland, closed shrubland, and grasslands) in regulating carbon sequestration. Furthermore, the study shows that ecosystem services are quite sensitive to droughts and floods, but buffers developed from previous year can play a significant role in mitigating this effect.

The model validation results successfully demonstrate that the model can be applied across central Europe (e.g. Germany). The simulated discharge had small model bias percentage and high regression values. Furthermore, the spatial and temporal variability of the discharge was modelled reasonably well with high NSE, KGE, R^2 and low P-bias for most watersheds (Table S3 - S4). Except for station Wasserthaleben, which had very high flow values leading to a P-bias equal to 131.8%, KGE of -1.48, and annual R^2 of 0.18. The poor performance of this individual station could be attributed to several possible reasons, including its relatively small surface area, the uncertainty of input data (soil parameters or climate data), underestimation of losses to groundwater, simplification of physical processes that estimate surface runoff, or the presence of prevalent unidentified dams in the watershed (Caldwell et al., 2012).



328 Simulated ET validated reasonably well against data from different eddy flux towers across the study area (Fig. 3).
 329 The largest discrepancy was found in Lackenberg station. Even though corrected ET values are used for validation,
 330 there might be uncertainties in correction factor (Pastorello et al., 2020) and inaccuracies in the observed data due to
 331 energy imbalance. For spatial analysis, the simulated ET was compared with MODIS data. The model values were
 332 low compared MODIS ET in southern and northwestern Germany, but high in mid-western and eastern Germany. The
 333 discrepancies between MODIS-ET and WaSSI ET could be attributed to multiple factors, i.e. the intrinsic limitations
 334 of the different algorithms used by the model and MODIS to estimate ET, uncertainty from the misclassification of
 335 land cover between the two datasets, uncertainties in the model's input data, uncertainties in MODIS's input data,
 336 exclusion of waterbodies in ET estimation by MODIS, and the role of interception in MODIS-ET estimation (Kim et
 337 al., 2012; Trambauer et al., 2014).

338 Furthermore, the model performance across different land covers showed that simulated GPP estimates capture forest
 339 biomes significantly well, except for the station in Lackenberg Forest. The model performance for the rest of the land
 340 covers was complex, but reasonable. For example, croplands had good model biases but low regression values;
 341 grasslands had poor model biases, but high regression estimates; wetlands are more complicated (see Table 1). The
 342 discrepancies in the results can be from 1) the model's inherent limitation i.e., lack of radiation in model PET leading
 343 to underestimation of GPP, 2) an insufficient number of eddy flux data for different land covers, and uncertainty in
 344 eddy flux GPP. The uncertainty of daily GPP can reach 15% to 20% (Falge et al., 2002; Hagen et al., 2006; Lasslop
 345 et al., 2010; Verma et al., 2014). Understanding uncertainties in eddy flux GPP is ongoing research. The mismatch of
 346 land cover and landscape heterogeneity at the evaluation sites between the model (watershed scale) and the eddy flux
 347 (single location) will reduce as more data becomes available with time (Verma et al., 2014). Lastly, the difference
 348 between spatial distribution of simulated GPP and remotely sensed GPP may be due to WUE parameters. They were
 349 derived from the global FLUXNET database, which might not have sufficient representation of certain ecosystems
 350 (e.g., wetlands and savannas) resulting in a bias of GPP estimation (G. Sun et al., 2011). Nevertheless, multiple studies
 351 have also shown that data from remote sensing tends to underestimate GPP (Z. Liu et al., 2015; Wang et al., 2017;
 352 Zhu et al., 2018).

353 The model helps determine the stocks and flows of ecosystem services across Germany. We found that Zink et al.
 354 (2016) and Huang et al. (2010) estimated similar annual ET and water scarcity patterns across Germany in their
 355 individual studies. The eastern region in Germany generally receives less precipitation, has high mean annual
 356 temperature, high ET from forests and low water yield, implying intense water use competition. The total water supply
 357 reported by German Environment Agency (UBA) was higher than the simulated results because WaSSI model does
 358 not take into account transboundary inflows (J. Arle et al., 2018). Furthermore, the southern region in Germany had
 359 slightly higher carbon uptake and sequestration values than the rest of the country. The distribution patterns of carbon
 360 sequestration were similar to carbon uptake because NEP and GPP have a linear relationship. Urban areas did not
 361 sequester any carbon but played a significant role in providing water supply. The distribution and management of land
 362 use and land cover determine how ecosystem services vary. To ensure adequate quantity and quality of services, like
 363 freshwater and natural sink of CO₂, land use decision-making must incorporate the assessment of currently available
 364 stocks and their actual value according to regional and national priorities. Based on historical data, the available
 365 stocks quantified in this study provide evidence to relevant stakeholders of different regions. Furthermore, the
 366 significance of minor land covers or ecosystems in terms of proportional coverage, such as wetlands, is also
 367 highlighted. Germany aims to become CO₂ neutral by 2045; synergies and tradeoffs of ecosystem services can be used
 368 to design land use policy that align with Sustainable Development Goals. A science-based approach will be necessary
 369 to leverage the potential of natural C sink to fix and offset carbon emissions.

370 As the frequency and intensity of periodic dry and wet spells change due to global warming so does their impact
 371 through drought and flood. In this work, we, quantified the response of water yield and carbon sequestration to extreme
 372 drought and high precipitation events across Germany. During the drought events of 2003 and 2018 the lack of
 373 precipitation, overall, had a direct negative impact on water yield and carbon sequestration. But it is interesting to see
 374 that soil is able to store water from the previous years which act as a buffer and provide limited relief during extreme
 375 drought events (Fig. 8). According to Ciais et al. (2005), a 30% reduction in carbon uptake was observed across Europe
 376 during the drought of 2003, while we estimated a reduction of around 8.8% for Germany. Europe-wide studies on the
 377 impacts of the 2018 drought event on carbon sequestration are presented by Thompson et al. (2020) and Smith et al.
 378 (2020). They found that the annual sequestration anomaly in 2018 across northern Europe was $0.02 \pm 0.02 \text{ PgC yr}^{-1}$



less compared to a 10-year European mean (Thompson et al., 2020). It was estimated that during the year 2018 an overall reduction in sequestration was around 57 TgC (Smith et al., 2020). However, a direct comparison between our research is difficult due to the difference in the spatial boundaries. In general, Germany has no shortage of water, however, a trend to have less precipitation during summer seasons or prolonged dry spells during main vegetation growing months can have substantial adverse effects on both surface water and groundwater supply. Temporary seasonal rainfall deficiency can cause significant losses of surface water supply and carbon sequestration, leading to dry conditions that negatively affect the yields and products from the agriculture and forestry sectors. For example, low soil water availability weakens forest health and favors bark beetle infestation, resulting in huge economic losses of timber values and forest areas in Germany over the last few years (Lausch et al., 2013; Zimmermann & Hoffmann, 2020). Therefore, land use transformation to adapt to climate change is indispensable to developing ecological resiliency based on an improved understanding of the role of various land covers in providing ecosystem services.

While this study provides valuable insights on response of water-carbon cycle to land cover and extreme events, it is limited by the scope of WaSSI Model. The monthly temporal resolution of the model prevents it from estimating peak flows accurately. The use of WUE to connect ET and carbon sequestration is limited due to insufficient eddy flux tower coverage. The lack of transboundary river flow and omission of crop rotation further limits the application of this model. In future, we plan to use WaSSI model across hydrological boundaries, apply projected climate data and projected landcover data to run simulations for different scenarios. The analysis will help us evaluate future changes in ecosystem services.

5. Conclusions

This study presents new insights into the relationship between water-carbon cycle and land cover, and the impacts of climate extremes across Germany. The model validation results holistically show that the simple water and carbon model could capture ecosystem services reasonably well at the national level. Furthermore, the spatial and temporal relationship between carbon and water highlighted that the eastern states of Germany are comparatively drier than the rest of the country because most of their precipitation is lost as ET. The average water yield across Germany ranges from 32 – 1478 mm yr⁻¹ and generates a total annual discharge of 84.86 billion m³ per year. Similarly, the average carbon sequestration ranges from 0 – 666 g C m⁻² yr⁻¹ and annually sequesters 106Tg C yr⁻¹. Our simulation results showed that croplands supply the largest percentage of available water, while DBF sequester the major share of carbon. The analysis also emphasized the critical role of minor land covers (e.g. wetlands, open shrubland, closed shrubland, and grasslands) in providing ecosystem services for carbon sequestration. The extreme events in 2003 and 2018 had a significant impact on ecosystem services at the national level. Moreover, the severe flood of 2013 also played a major role on a regional scale in the Elbe and Danube River basins. This rigorously verified model provides confidence that the model can be used to strategic applications for developing Nature-based Solutions (NbS), which will be helpful for Germany to meet its net-zero carbon emissions by 2050. In the future, we aim to concentrate our research efforts on understanding how land use land cover change or landscape transformation will affect water yield and carbon sequestration across different watersheds for climate adaptation.



414 **6. Acknowledgment**

415 This work was supported by the German Academic Exchange Service (DAAD) PPP Grant (Projekt-ID: 57510261).
416 We appreciate the funding support from UNU-FLORES and the generous support provided by the US partner – the
417 Southern Research Station of the United States Forest Service. We also would like to thank the Thünen Institute of
418 Forest Ecosystems for collaboration.

419 **7. Data Availability**

420 Model software (N. Liu, 2021), output data (Pyarali, 2024b) and corresponding watershed shapefile (Pyarali, 2024a)
421 used and prepared in this study are available open source via figshare and can be access from the links in reference
422 list.

423 **8. Author Contributions**

424 *Karim Pyarali*: Writing, review & editing manuscript, Methodology, Investigation, Data curation, Conceptualization.
425 *Lulu Zhang*: Review, Supervision, Methodology, Funding acquisition, Conceptualization. *Ge Sun*: Review,
426 Supervision, Methodology, Conceptualization. *Ning Liu*: Review, Data curation, Methodology. *Abdulhakeem Al-*
427 *Qubati*: Review, Data curation, Methodology.

428 **9. Competing Interests:**

429 The authors declare that they have no known competing financial interests or personal relationships that could have
430 appeared to influence the work reported in this paper.



431 **10. Reference**

- 432 Allan, A., Soltani, A., Abdi, M. H., & Zarei, M. (2022). Driving Forces behind Land Use and Land Cover Change: A
433 Systematic and Bibliometric Review. *Land*, 11(8), 1222. <https://doi.org/10.3390/land11081222>
- 434 Al-Qubati, A., Zhang, L., & Pyarali, K. (2023). Climatic drought impacts on key ecosystem services of a low mountain
435 region in Germany. *Environmental Monitoring and Assessment*, 195(7), 800. [https://doi.org/10.1007/s10661-](https://doi.org/10.1007/s10661-023-11397-1)
436 023-11397-1
- 437 Anderson, R. M., Koren, V. I., & Reed, S. M. (2006). Using SSURGO data to improve Sacramento Model a priori
438 parameter estimates. *Journal of Hydrology*, 320(1–2), 103–116.
439 <https://doi.org/10.1016/J.JHYDROL.2005.07.020>
- 440 Arowolo, A. O., Deng, X., Olatunji, O. A., & Obayelu, A. E. (2018). Assessing changes in the value of ecosystem
441 services in response to land-use/land-cover dynamics in Nigeria. *Science of The Total Environment*, 636, 597–
442 609. <https://doi.org/10.1016/j.scitotenv.2018.04.277>
- 443 Averyt, K., Fisher, J., Huber-Lee, A., Lewis, A., Macknick, J., Madden, N., Rogers, J., & Tellinghuisen, S. (2011).
444 *Freshwater Use by U.S. Power Plants. Electricity's Thirst for a Precious Resource*.
- 445 Beer, C., Reichstein, M., Ciais, P., Farquhar, G. D., & Papale, D. (2007). Mean annual GPP of Europe derived from
446 its water balance. *Geophysical Research Letters*, 34(5). <https://doi.org/10.1029/2006GL029006>
- 447 Brown de Colstoun, E. C., C. Huang, P. Wang, J. C. Tilton, B. Tan, J. Phillips, S. Niemczura, P.-Y. Ling, & R. E.
448 Wolfe. (2017). *Global Man-made Impervious Surface (GMIS) Dataset From Landsat, v1: Global High*
449 *Resolution Urban Data from Landsat [Dataset]*. Palisades, NY: NASA Socioeconomic Data and Applications
450 Center (SEDAC).
- 451 Büttner, G., Kosztra, B., Maucha, G., Pataki, R., Kleeschulte, S., Hazeu, G., Vittek, M., Schröder, C., & Littkopf, A.
452 (2021). *Copernicus Land Monitoring Service CORINE Land Cover (User Manual)*.
453 <https://land.copernicus.eu/pan-european/corine-land-cover/clc2018?tab=mapview>
- 454 Caldwell, P., Muldoon, C., Ford-Miniat, C., Cohen, E., Krieger, S., Sun, G., McNulty, S., & Bolstad, P. V. (2014).
455 *Quantifying the role of National Forest System lands in providing surface drinking water supply for the Southern*
456 *United States*. <https://doi.org/10.2737/SRS-GTR-197>
- 457 Caldwell, P., Sun, G., McNulty, S. G., Cohen, E., & Moore Myers, J. a. (2011). Modeling impacts of environmental
458 change on ecosystem services across the conterminous United States. *The Fourth Interagency Conference on*
459 *Research in the Watersheds*, Fairbanks, AK, USA.
460 http://admin.forestthreats.org/products/publications/Modeling_impacts_of_environmental_change.pdf
- 461 Caldwell, P. V., Sun, G., McNulty, S. G., Cohen, E. C., & Moore Myers, J. A. (2012). Impacts of impervious cover,
462 water withdrawals, and climate change on river flows in the conterminous US. *Hydrology and Earth System*
463 *Sciences*, 16(8), 2839–2857. <https://doi.org/10.5194/hess-16-2839-2012>
- 464 Camacho, F., & Cernicharo, J. (2014). Gio Global Land Component - Lot I "Operation of the Global Land
465 Component". In *Algorithm Theoretical Basis Document, Issue 11.01*.
466 http://land.copernicus.eu/global/sites/default/files/products/GIOGL1_ATBD_SAV1_I1.01.pdf
- 467 Cheng, L., Zhang, L., Wang, Y. P., Canadell, J. G., Chiew, F. H. S., Beringer, J., Li, L., Miralles, D. G., Piao, S., &
468 Zhang, Y. (2017). Recent increases in terrestrial carbon uptake at little cost to the water cycle. *Nature*
469 *Communications* 2017 8:1, 8(1), 1–10. <https://doi.org/10.1038/s41467-017-00114-5>
- 470 Ciais, P., Reichstein, M., Viovy, N., Granier, A., Ogée, J., Allard, V., Aubinet, M., Buchmann, N., Bernhofer, C.,
471 Carrara, A., Chevallier, F., De Noblet, N., Friend, A. D., Friedlingstein, P., Grünwald, T., Heinesch, B.,
472 Keronen, P., Knohl, A., Krinner, G., ... Valentini, R. (2005). Europe-wide reduction in primary productivity



- 473 caused by the heat and drought in 2003. *Nature* 2005 437:7058, 437(7058), 529–533.
474 <https://doi.org/10.1038/nature03972>
- 475 Cui, F., Wang, B., Zhang, Q., Tang, H., De Maeyer, P., Hamdi, R., & Dai, L. (2021). Climate change versus land-use
476 change—What affects the ecosystem services more in the forest-steppe ecotone? *Science of The Total*
477 *Environment*, 759, 143525. <https://doi.org/10.1016/j.scitotenv.2020.143525>
- 478 Donmez, C., Sahingoz, M., Paul, C., Cilek, A., Hoffmann, C., Berberoglu, S., Webber, H., & Helming, K. (2024).
479 Climate change causes spatial shifts in the productivity of agricultural long-term field experiments. *European*
480 *Journal of Agronomy*, 155, 127121. <https://doi.org/10.1016/j.eja.2024.127121>
- 481 DWD. (2018). *Grids of monthly averaged daily air temperature (2m) over Germany [Dataset]*.
482 https://opendata.dwd.de/climate_environment/CDC/grids_germany/monthly/
- 483 EEA. (2021). *CLC 2018 — Copernicus Land Monitoring Service [Dataset]*. [https://land.copernicus.eu/pan-](https://land.copernicus.eu/pan-european/corine-land-cover/clc2018)
484 [european/corine-land-cover/clc2018](https://land.copernicus.eu/pan-european/corine-land-cover/clc2018)
- 485 Eisenreich, S. J. (2005). *Climate Change and the European Water Dimension. A report to the European Water*
486 *Directors 2005. EU Report No. 21553*. [https://cetesb.sp.gov.br/proclima/2005/05/09/climate-change-and-the-](https://cetesb.sp.gov.br/proclima/2005/05/09/climate-change-and-the-european-water-dimension-a-report-to-the-european-water-directors/)
487 [european-water-dimension-a-report-to-the-european-water-directors/](https://cetesb.sp.gov.br/proclima/2005/05/09/climate-change-and-the-european-water-dimension-a-report-to-the-european-water-directors/)
- 488 Falge, E., Baldocchi, D., Tenhunen, J., Aubinet, M., Bakwin, P., Berbigier, P., Bernhofer, C., Burba, G., Clement, R.,
489 Davis, K. J., Elbers, J. A., Goldstein, A. H., Grelle, A., Granier, A., Gumundsson, J., Hollinger, D., Kowalski,
490 A. S., Katul, G., Law, B. E., ... Wofsy, S. (2002). Seasonality of ecosystem respiration and gross primary
491 production as derived from FLUXNET measurements. *Agricultural and Forest Meteorology*, 113(1–4), 53–74.
492 [https://doi.org/10.1016/S0168-1923\(02\)00102-8](https://doi.org/10.1016/S0168-1923(02)00102-8)
- 493 Fang, Y., Sun, G., Caldwell, P., McNulty, S. G., Noormets, A., Domec, J. C., King, J., Zhang, Z., Zhang, X., Lin, G.,
494 Zhou, G., Xiao, J., & Chen, J. (2016). Monthly land cover-specific evapotranspiration models derived from
495 global eddy flux measurements and remote sensing data. *Ecohydrology*, 9(2), 248–266.
496 <https://doi.org/10.1002/eco.1629>
- 497 *Fourth Federal Forest Inventory 2022*. (2024). [https://www.bundeswaldinventur.de/vierte-bundeswaldinventur-](https://www.bundeswaldinventur.de/vierte-bundeswaldinventur-2022/vorwort)
498 [2022/vorwort](https://www.bundeswaldinventur.de/vierte-bundeswaldinventur-2022/vorwort)
- 499 Gentine, P., Green, J. K., Guérin, M., Humphrey, V., Seneviratne, S. I., Zhang, Y., & Zhou, S. (2019). Coupling
500 between the terrestrial carbon and water cycles—a review. *Environmental Research Letters*, 14(8), 083003.
501 <https://doi.org/10.1088/1748-9326/AB22D6>
- 502 Gutsch, M., Lasch-Born, P., Kollas, C., Suckow, F., & Reyer, C. P. O. (2018). Balancing trade-offs between ecosystem
503 services in Germany's forests under climate change. *Environmental Research Letters*, 13(4), 045012.
504 <https://doi.org/10.1088/1748-9326/aab4e5>
- 505 Hagen, S. C., Braswell, B. H., Linder, E., Frolking, S., Richardson, A. D., & Hollinger, D. Y. (2006). Statistical
506 uncertainty of eddy flux - Based estimates of gross ecosystem carbon exchange at Howland Forest, Maine.
507 *Journal of Geophysical Research Atmospheres*, 111(8), 1–12. <https://doi.org/10.1029/2005JD006154>
- 508 Hasan, S. S., Zhen, L., Miah, Md. G., Ahamed, T., & Samie, A. (2020). Impact of land use change on ecosystem
509 services: A review. *Environmental Development*, 34, 100527. <https://doi.org/10.1016/j.envdev.2020.100527>
- 510 Huang, S., Krysanova, V., Österle, H., & Hattermann, F. F. (2010). Simulation of spatiotemporal dynamics of water
511 fluxes in Germany under climate change. *Hydrological Processes*, 24(23), 3289–3306.
512 <https://doi.org/10.1002/HYP.7753>
- 513 J. Arle, H. Bartel, C. Baumgarten, A. Bertram, R. Wolter, G. Winkelmann-Oei, & C. Winde. (2018). *Water Resource*
514 *Management in Germany: Fundamentals, Pressures, Measures*.
515 <https://www.umweltbundesamt.de/en/publikationen/water-resource-management-in-germany>



- 516 Jung, M., Reichstein, M., Schwalm, C. R., Huntingford, C., Sitch, S., Ahlström, A., Arneth, A., Camps-Valls, G.,
517 Ciais, P., Friedlingstein, P., Gans, F., Ichii, K., Jain, A. K., Kato, E., Papale, D., Poulter, B., Raduly, B.,
518 Rödenbeck, C., Tramontana, G., ... Zeng, N. (2017). Compensatory water effects link yearly global land CO₂
519 sink changes to temperature. *Nature* 2017 541:7638, 541(7638), 516–520. <https://doi.org/10.1038/nature20780>
- 520 Kaspar, F., Müller-Westermeier, G., Penda, E., Mächel, H., Zimmermann, K., Kaiser-Weiss, A., & Deutschländer, T.
521 (2013). Monitoring of climate change in Germany – data, products and services of Germany’s National Climate
522 Data Centre. *Advances in Science and Research*, 10(1), 99–106. <https://doi.org/10.5194/asr-10-99-2013>
- 523 Keil, M. (2017). *CORINE Land Cover products for Germany* (Issue January).
524 [https://www.dlr.de/eoc/Portaldata/60/Resources/dokumente/6_anw_land/CORINE_Land_Cover_products_for](https://www.dlr.de/eoc/Portaldata/60/Resources/dokumente/6_anw_land/CORINE_Land_Cover_products_for_Germany_at_DFD.pdf)
525 [_Germany_at_DFD.pdf](https://www.dlr.de/eoc/Portaldata/60/Resources/dokumente/6_anw_land/CORINE_Land_Cover_products_for_Germany_at_DFD.pdf)
- 526 Kim, H. W., Hwang, K., Mu, Q., Lee, S. O., & Choi, M. (2012). Validation of MODIS 16 global terrestrial
527 evapotranspiration products in various climates and land cover types in Asia. *KSCE Journal of Civil*
528 *Engineering*, 16(2), 229–238. <https://doi.org/10.1007/s12205-012-0006-1>
- 529 Lasslop, G., Reichstein, M., Papale, D., Richardson, A., Arneth, A., Barr, A., Stoy, P., & Wohlfahrt, G. (2010).
530 Separation of net ecosystem exchange into assimilation and respiration using a light response curve approach:
531 Critical issues and global evaluation. *Global Change Biology*, 16(1), 187–208. [https://doi.org/10.1111/j.1365-](https://doi.org/10.1111/j.1365-2486.2009.02041.x)
532 [2486.2009.02041.x](https://doi.org/10.1111/j.1365-2486.2009.02041.x)
- 533 Lausch, A., Heurich, M., & Fahse, L. (2013). Spatio-temporal infestation patterns of *Ips typographus* (L.) in the
534 Bavarian Forest National Park, Germany. *Ecological Indicators*, 31, 73–81.
535 <https://doi.org/10.1016/J.ECOLIND.2012.07.026>
- 536 Law, B. E., Falge, E., Gu, L., Baldocchi, D. D., Bakwin, P., Berbigier, P., Davis, K., Dolman, A. J., Falk, M., Fuentes,
537 J. D., Goldstein, A., Granier, A., Grelle, A., Hollinger, D., Janssens, I. A., Jarvis, P., Jensen, N. O., Katul, G.,
538 Mahli, Y., ... Wofsy, S. (2002). Environmental controls over carbon dioxide and water vapor exchange of
539 terrestrial vegetation. *Agricultural and Forest Meteorology*, 113(1–4), 97–120. [https://doi.org/10.1016/S0168-](https://doi.org/10.1016/S0168-1923(02)00104-1)
540 [1923\(02\)00104-1](https://doi.org/10.1016/S0168-1923(02)00104-1)
- 541 Liu, N. (2017). *Changes in Water and Carbon in Australian Vegetation in Response to Climate Change* [Murdoch
542 University]. <https://researchrepository.murdoch.edu.au/id/eprint/40206/>
- 543 Liu, N. (2021). *R-based Water Supply Stress Index (rWaSSI) model [Software]*.
544 <https://sites.google.com/view/rwassi/home?authuser=0>
- 545 Liu, N., Dobbs, G. R., Caldwell, P. V., Miniati, C. F., Bolstad, P. V., Nelson, S., & Sun, G. (2020). *Quantifying the*
546 *role of State and private forest lands in providing surface drinking water supply for the Southern United States*.
547 <https://doi.org/10.2737/SRS-GTR-248>
- 548 Liu, N., SUN, P.-S., Liu, S.-R., & Sun, G. (2013). Determination of spatial scale of response unit for WASSI-C eco-
549 hydrological model—a case study on the upper Zagunao River watershed of China. *Chinese Journal of Plant*
550 *Ecology*. <https://doi.org/10.3724/SP.J.1258.2013.00000>
- 551 Liu, Z., Shao, Q., & Liu, J. (2015). The performances of MODIS-GPP and -ET products in China and their sensitivity
552 to input data (FPAR/LAI). *Remote Sensing*, 7(1), 135–152. <https://doi.org/10.3390/rs70100135>
- 553 Margulis, S. A., Wood, E. F., & Troch, P. A. (2006). The Terrestrial Water Cycle: Modeling and Data Assimilation
554 across Catchment Scales. *Journal of Hydrometeorology*, 7(3), 309–311. <https://doi.org/10.1175/JHM999.1>
- 555 McCabe, G. J., & Wolock, D. M. (1999). GENERAL-CIRCULATION-MODEL SIMULATIONS OF FUTURE
556 SNOWPACK IN THE WESTERN UNITED STATES1. *JAWRA Journal of the American Water Resources*
557 *Association*, 35(6), 1473–1484. <https://doi.org/10.1111/J.1752-1688.1999.TB04231.X>



- McIntyre, S., Cohen, E., Sun, G., & Caldwell, P. (2016). HYDROLOGIC MODELING FOR WATER RESOURCE ASSESSMENT IN A DEVELOPING COUNTRY: THE RWANDA CASE STUDY. *USDA FOREST SERVICE*. <https://www.fs.usda.gov/treesearch/pubs/53039>
- Morales, P., Sykes, M. T., Prentice, I. C., Smith, P., Smith, B., Bugmann, H., Zierl, B., Friedlingstein, P., Viovy, N., Sabaté, S., Sánchez, A., Pla, E., Gracia, C. A., Sitch, S., Arneth, A., & Ogee, J. (2005). Comparing and evaluating process-based ecosystem model predictions of carbon and water fluxes in major European forest biomes. *Global Change Biology*, 11(12), 2211–2233. <https://doi.org/10.1111/J.1365-2486.2005.01036.X>
- Pandey, B., & Ghosh, A. (2023). Urban ecosystem services and climate change: a dynamic interplay. *Frontiers in Sustainable Cities*, 5. <https://doi.org/10.3389/frsc.2023.1281430>
- Pastorello, G., Trotta, C., Canfora, E., Chu, H., Christianson, D., Cheah, Y. W., Poindexter, C., Chen, J., Elbashandy, A., Humphrey, M., Isaac, P., Polidori, D., Ribeca, A., van Ingen, C., Zhang, L., Amiro, B., Ammann, C., Arain, M. A., Ardö, J., ... Papale, D. (2020). The FLUXNET2015 dataset and the ONEFlux processing pipeline for eddy covariance data [Dataset]. *Scientific Data*, 7(1), 225. <https://doi.org/10.1038/s41597-020-0534-3>
- Potter, C., & Pass, S. (2024). Changes in the net primary production of ecosystems across Western Europe from 2015 to 2022 in response to historic drought events. *Carbon Balance and Management*, 19(1), 32. <https://doi.org/10.1186/s13021-024-00279-9>
- Prescher, A.-K., Grünwald, T., & Bernhofer, C. (2010). Land use regulates carbon budgets in eastern Germany: From NEE to NBP. *Agricultural and Forest Meteorology*, 150(7–8), 1016–1025. <https://doi.org/10.1016/j.agrformet.2010.03.008>
- Pyarali, K. (2024a). *Germany Watershed Delineation [Dataset]*. Figshare. <https://doi.org/https://doi.org/10.6084/m9.figshare.25053599.v1>
- Pyarali, K. (2024b). *WaSSI Model Output [Dataset]*. Figshare. <https://doi.org/https://doi.org/10.6084/m9.figshare.25053641.v1>
- Running, S. W., Mu, Q., Zhao, M., & Moreno, A. (2019a). *User's Guide Daily GPP and Annual NPP (MOD17A2H/A3H) and Year-end Gap-Filled (MOD17A2HGF/A3HGF) Products [Dataset]*. <https://lpdaac.usgs.gov/products/mod17a2hgf006/>
- Running, S. W., Mu, Q., Zhao, M., & Moreno, A. (2019b). *User's Guide MODIS Global Terrestrial Evapotranspiration (ET) Product NASA Earth Observing System MODIS Land Algorithm (For Collection 6) [Dataset]*. <https://doi.org/10.5067/MODIS/MOD16A2GF.006>
- Salerno, F., Gaetano, V., & Gianni, T. (2018). Urbanization and climate change impacts on surface water quality: Enhancing the resilience by reducing impervious surfaces. *Water Research*, 144, 491–502. <https://doi.org/10.1016/j.watres.2018.07.058>
- Schröter, D., Zebisch, M., & Grothmann, T. (2005). *Climate Change in Germany-Vulnerability and Adaptation of Climate-Sensitive Sectors*. https://www.researchgate.net/publication/232071870_Climate_Change_in_Germany-Vulnerability_and_Adaptation_of_Climate-Sensitive_Sectors
- Schumacher, E. (2022, January 10). *Natural disasters cost \$280 billion in 2021: German insurance firm | News | DW / 10.01.2022*. <https://www.dw.com/en/natural-disasters-cost-280-billion-in-2021-german-insurance-firm/a-60378575>
- Smets, B., Swinnen, E., & Van Hoolst, R. (2019). Product User Manual: Dry Matter Productivity and Gross Dry Matter Productivity. Version 2. Collection 1km. In *Copernicus Global Land Services [Dataset]*. <https://land.copernicus.eu/global/products/dmp>



- 600 Smith, N. E., Kooijmans, L. M. J., Koren, G., Van Schaik, E., Van Der Woude, A. M., Wanders, N., Ramonet, M.,
601 Xueref-Remy, I., Siebicke, L., Manca, G., Brümmner, C., Baker, I. T., Haynes, K. D., Luijkx, I. T., & Peters, W.
602 (2020). Spring enhancement and summer reduction in carbon uptake during the 2018 drought in northwestern
603 Europe. *Philosophical Transactions of the Royal Society B*, 375(1810).
604 <https://doi.org/10.1098/RSTB.2019.0509>
- 605 Sun, G., Caldwell, P., Noormets, A., McNulty, S. G., Cohen, E., Myers, J. M., Domec, J.-C., Treasure, E., Mu, Q.,
606 Xiao, J., John, R., & Chen, J. (2011). Upscaling key ecosystem functions across the conterminous United States
607 by a water-centric ecosystem model. *Journal of Geophysical Research: Biogeosciences*, 116(G3).
608 <https://doi.org/10.1029/2010JG001573>
- 609 Sun, G., Wei, X., Hao, L., Sanchis, M. G., Hou, Y., Yousefpour, R., Tang, R., & Zhang, Z. (2023). Forest hydrology
610 modeling tools for watershed management: A review. *Forest Ecology and Management*, 530(4), 120755-.
611 <https://doi.org/10.1016/J.FORECO.2022.120755>
- 612 Sun, S., Sun, G., Caldwell, P., McNulty, S. G., Cohen, E., Xiao, J., & Zhang, Y. (2015). Drought impacts on ecosystem
613 functions of the U.S. National Forests and Grasslands: Part I evaluation of a water and carbon balance model.
614 *Forest Ecology and Management*, 353, 260–268. <https://doi.org/10.1016/j.foreco.2015.03.054>
- 615 Thompson, R. L., Broquet, G., Gerbig, C., Koch, T., Lang, M., Monteil, G., Munassar, S., Nickless, A., Scholze, M.,
616 Ramonet, M., Karstens, U., Van Schaik, E., Wu, Z., & Rödenbeck, C. (2020). Changes in net ecosystem
617 exchange over Europe during the 2018 drought based on atmospheric observations. *Philosophical Transactions
618 of the Royal Society B*, 375(1810). <https://doi.org/10.1098/RSTB.2019.0512>
- 619 Trambauer, P., Dutra, E., Maskey, S., Werner, M., Pappenberger, F., Van Beek, L. P. H., & Uhlenbrook, S. (2014).
620 Comparison of different evaporation estimates over the African continent. *Hydrology and Earth System
621 Sciences*, 18(1), 193–212. <https://doi.org/10.5194/hess-18-193-2014>
- 622 Turner, D. P., Ritts, W. D., Cohen, W. B., Gower, S. T., Running, S. W., Zhao, M., Costa, M. H., Kirschbaum, A. A.,
623 Ham, J. M., Saleska, S. R., & Ahl, D. E. (2006). Evaluation of MODIS NPP and GPP products across multiple
624 biomes. *Remote Sensing of Environment*, 102(3–4), 282–292. <https://doi.org/10.1016/j.rse.2006.02.017>
- 625 Ungaro, F., Schwartz, C., & Piore, A. (2021). Ecosystem services indicators dataset for the utilized agricultural area
626 of the Märkisch-Oderland District-Brandenburg, Germany. *Data in Brief*, 34, 106645.
627 <https://doi.org/10.1016/j.dib.2020.106645>
- 628 Velpuri, N. M., Senay, G. B., Singh, R. K., Bohms, S., & Verdin, J. P. (2013). A comprehensive evaluation of two
629 MODIS evapotranspiration products over the conterminous United States: Using point and gridded FLUXNET
630 and water balance ET. *Remote Sensing of Environment*, 139, 35–49. <https://doi.org/10.1016/j.rse.2013.07.013>
- 631 Verger, A., Descals, A., Benhadj, I., & Claes, P. (2018). *Product User Guide and Specification: CDR VGT-based LAI
632 and fAPAR v1.0 [Dataset]*. [http://datastore.copernicus-climate.eu/c3s/published-forms/c3sprod/satellite-soil-
633 moisture/product-user-guide-v2.3.pdf](http://datastore.copernicus-climate.eu/c3s/published-forms/c3sprod/satellite-soil-moisture/product-user-guide-v2.3.pdf)
- 634 Verma, M., Friedl, M. A., Richardson, A. D., Kiely, G., Cescatti, A., Law, B. E., Wohlfahrt, G., Gielen, B., Rouspard,
635 O., Moors, E. J., Toscano, P., Vaccari, F. P., Gianelle, D., Bohrer, G., Varlagin, A., Buchmann, N., Van Gorsel,
636 E., Montagnani, L., & Propastin, P. (2014). Remote sensing of annual terrestrial gross primary productivity from
637 MODIS: An assessment using the FLUXNET la Thuile data set. *Biogeosciences*, 11(8), 2185–2200.
638 <https://doi.org/10.5194/bg-11-2185-2014>
- 639 Wang, L., Zhu, H., Lin, A., Zou, L., Qin, W., & Du, Q. (2017). Evaluation of the latest MODIS GPP products across
640 multiple biomes using global eddy covariance flux data. *Remote Sensing*, 9(5).
641 <https://doi.org/10.3390/rs9050418>



- Williams, I. N., Torn, M. S., Riley, W. J., & Wehner, M. F. (2014). Impacts of climate extremes on gross primary production under global warming. *Environmental Research Letters*, 9(9), 094011. <https://doi.org/10.1088/1748-9326/9/9/094011>
- Wu, S., Tetzlaff, D., Goldammer, T., & Soulsby, C. (2021). Hydroclimatic variability and riparian wetland restoration control the hydrology and nutrient fluxes in a lowland agricultural catchment. *Journal of Hydrology*, 603, 126904. <https://doi.org/10.1016/j.jhydrol.2021.126904>
- Zeng, Z., Piao, S., Li, L. Z. X., Wang, T., Ciais, P., Lian, X., Yang, Y., Mao, J., Shi, X., & Myneni, R. B. (2018). Impact of Earth Greening on the Terrestrial Water Cycle. *Journal of Climate*, 31(7), 2633–2650. <https://doi.org/10.1175/JCLI-D-17-0236.1>
- Zhang, J., Zhang, Y., Sun, G., Song, C., Li, J., Hao, L., & Liu, N. (2022). Climate Variability Masked Greening Effects on Water Yield in the Yangtze River Basin During 2001–2018. *Water Resources Research*, 58(1), e2021WR030382. <https://doi.org/10.1029/2021WR030382>
- Zhang, L., Cheng, L., Chiew, F., & Fu, B. (2018). Understanding the impacts of climate and landuse change on water yield. *Current Opinion in Environmental Sustainability*, 33, 167–174. <https://doi.org/10.1016/J.COSUST.2018.04.017>
- Zhang, Y., Song, C., Sun, G., Band, L. E., McNulty, S., Noormets, A., Zhang, Q., & Zhang, Z. (2016). Development of a coupled carbon and water model for estimating global gross primary productivity and evapotranspiration based on eddy flux and remote sensing data. *Agricultural and Forest Meteorology*, 223, 116–131. <https://doi.org/10.1016/J.AGRFORMET.2016.04.003>
- Zhang, Y., Zhang, Z., Reed, S., & Koren, V. (2011). An enhanced and automated approach for deriving a priori SAC-SMA parameters from the soil survey geographic database. *Computers & Geosciences*, 37(2), 219–231. <https://doi.org/10.1016/J.CAGEO.2010.05.016>
- Zhu, X., Pei, Y., Zheng, Z., Dong, J., Zhang, Y., Wang, J., Chen, L., Doughty, R. B., Zhang, G., & Xiao, X. (2018). Underestimates of grassland gross primary production in MODIS standard products. *Remote Sensing*, 10(11). <https://doi.org/10.3390/rs10111771>
- Zimmermann, S., & Hoffmann, K. (2020). Evaluating the capabilities of Sentinel-2 data for large-area detection of bark beetle infestation in the Central German Uplands. <https://doi.org/10.1117/1.JRS.14.024515>, 14(2), 024515. <https://doi.org/10.1117/1.JRS.14.024515>
- Zink, M., Kumar, R., Cuntz, M., & Samaniego, L. (2016). A High-Resolution Dataset of Water Fluxes and States for Germany Accounting for Parametric Uncertainty. *Hydrology and Earth System Sciences Discussions*, September, 1–29. <https://doi.org/10.5194/hess-2016-443>